OE Optical Engineering

RESEARCH PAPER

Focal plane analysis of optical power-related metrics for atmospheric turbulence-affected laser beams

Italo Toselli*
Fraunhofer Institute of Optronics, System Technologies and Image Exploitation, Fraunhofer IOSB, Ettlingen, Germany

ABSTRACT. The analysis of budget link and free space optical system performances requires the calculation of several metrics of the atmospheric turbulence-affected collected light. In this work, assuming the collected light is focused into an optical fiber or over a sensor positioned in the focal plane, we use the ABCD ray-matrix representation to calculate the impact of atmospheric turbulence on the power in the fiber or power over the sensor. Calculation of such metrics requires the knowledge of the transmitted average power that enters the receiver aperture (power in the bucket) and the long-term beam spread in the focal plane, from which the Strehl ratio can be obtained.

 [DOI: 10.1117/1.OE.63.4.041208]

Keywords: atmospheric turbulence; focal plane; long-term beam spread; optical system performances; power in the fiber; power in the bucket; Strehl ratio; budget link

Paper 20230926SS received Oct. 18, 2023; revised Dec. 12, 2023; accepted Dec. 18, 2023; published Jan. 9, 2024.

1 Introduction

The parameter that characterizes the mean radius of a Gaussian beam after propagation through optical turbulence over a distance L from the source or transmitter is referred to as the long-term beam spread.[1–3] This parameter holds significance in various applications, particularly in directed energy scenarios. In the realm of free-space optical communications, it becomes essential to extend the theoretical modeling of the long-term beam spread to the focal plane, where an optical detector or an optical fiber is commonly positioned.[4]

This paper extends the analysis of the long-term beam spread and Strehl ratio (SR) in the focal plane, as explained in Ref. 4, to conduct an examination of other optical power-related important metrics for budget link calculations. In particular, we calculate the average power in the bucket (PIB) captured by the receiver aperture and, depending on the presence of a fiber or a sensor in the focal plane, the average power into the fiber (PIF) or the average power over the sensor (POS).

We perform this analysis for Gaussian beams with general geometries, encompassing focused, collimated, and divergent configurations. Our methodology relies on the ABCD matrix representation[1] and accommodates scenarios where turbulence can deviate from the assumptions of the Kolmogorov model.[2]

*Address all correspondence to Italo Toselli, italo.toselli@iosb.fraunhofer.de

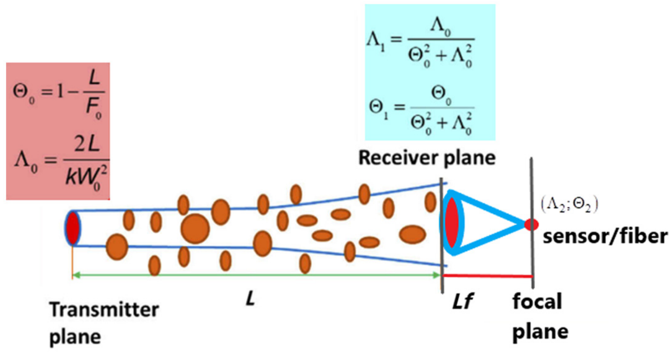

Fig. 1 Free space optical communication scheme.

2 Kolmogorov and Non-Kolmogorov Turbulence

Let us focus on the following power law-dependent non-Kolmogorov power spectrum:[2]

$$\Phi_n(\kappa, \alpha) = A(\alpha) \cdot \tilde{C}_n^2 \cdot \kappa^{-\alpha} \quad \text{with } 3 < \alpha < 4, \tag{1}$$

where $A(\alpha) = \frac{\Gamma(\alpha-1)}{4\pi^2} \cos(\alpha\frac{\pi}{2})$, $\vec{\kappa} \equiv (\kappa_x, \kappa_y, \kappa_z)$ is the spatial wavenumber vector, α is the power law, $\tilde{C}_n^2 = \beta(\alpha) \cdot C_n^2$ is the generalized structure parameter with units $[m^{3-\alpha}]$, $\beta(\alpha)$ is a constant depending on α and has units $[m^{11/3-\alpha}]$, and symbol $\Gamma(x)$ denotes the Gamma function. When power law assumes value $\alpha = 11/3$, the generalized structure parameter reduces to the structure parameter C_n^2 with units $[m^{-2/3}]$ and Eq. (1) reduces to the Kolmogorov power spectrum, $\Phi_n(\kappa) = 0.033 \cdot C_n^2 \cdot \kappa^{-11/3}$.

The schematic of a free space optical communication system is shown in Fig. 1. A Gaussian beam with spot radius W_0 exits the transmitter aperture with geometry defined by a couple of beam parameters $(\Theta_0 = 1 - \frac{L}{F_0}; \Lambda_0 = \frac{2L}{kW_0^2})$.

Here L is the path length, F_0 is the radius of curvature of the wavefront at the transmitter, and k is the wavenumber. After propagation, the beam is captured at the receiver aperture by a collecting lens of diameter D_G. The beam on the collecting lens has geometry described by $\Theta_1 = \frac{\Theta_0}{\Lambda_0^2+\Theta_0^2}; \Lambda_1 = \frac{\Lambda_0}{\Lambda_0^2+\Theta_0^2}$ and it is focused at distance L_f behind the lens, where a detector or an optical fiber is located.

Note that here we consider a hard aperture with diameter D_G related to the soft aperture Gaussian lens of radius W_G by the known expression $D_G^2 = 8 \cdot W_G^2$ (see Ref. 1). The beam in the focal plane has the geometry $(\Lambda_2 = \frac{L}{L_f} \cdot \frac{1}{\Lambda_1+\Omega_G}; \Theta_2 = 0)$, where $\Omega_G = \frac{2L}{kW_G^2}$ and $F_G = L_f$ is the focal length of the collecting lens. The diffraction-limited beam spot radius, W_2 in the focal plane is related to the diffraction parameter $\Lambda_2 = \frac{2L_f}{kW_2^2}$, therefore, $W_2 = \sqrt{\frac{2L_f}{k\Lambda_2}}$.

Note that all the geometric parameters, $\Theta_0, \Lambda_0; \Theta_1, \Lambda_1$ and Θ_2, Λ_2 are free space parameters, however they enter the equation describing the change in the on-axis mean irradiance in the focal plane after propagation in turbulence, Eq. (8).

3 Long Term Beam Spread Analysis in the Focal Plane

The long-term beam spread is the parameter that physically describes the mean radius of the Gaussian beam after its propagation in optical turbulence. The long-term spot radius in the focal plane can be defined as in Refs. 1, 2, and 4

$$W_{LT,f} = W_2 \cdot \left(1 + T_{\text{focal}}\right)^{\frac{3}{5}}, \tag{2}$$

where T_{focal} describes the change in the on-axis mean irradiance in the focal plane and characterizes the beam spread due to turbulence on a long-term average. Indeed, such a term includes the spread due to beam wander and small-scale turbulence cells diffraction.

As previously introduced, to calculate T_{focal} we use the ABCD ray-matrix representation shown in Ref. 1, and we neglect the effect of turbulence on the beam behind the lens (beam path from the lens to the detector). Under this condition, we use two statistical terms[1]

$$E_1(0{,}0)_f = -2\pi^2 k^2 L \cdot \int_0^\infty \kappa \cdot \Phi_n(\kappa) \cdot \mathrm{d}\kappa, \tag{3}$$

and

$$E_2(0{,}0)_f = 4\pi^2 k^2 L \cdot \int_0^1 \int_0^\infty \kappa \cdot \Phi_n(\kappa) \cdot \exp\left\{-i\frac{\kappa^2}{2\,k}[\gamma_1 B_1(\xi) - \gamma_1^* B_1^*(\xi)]\right\}\mathrm{d}\kappa\,\mathrm{d}\xi, \tag{4}$$

where $k = 2\pi/\lambda$ is wave number, λ is the wave length, $\xi = 1 - z/L$ is the normalized z-distance.

For a beam focused on the photodetector/optical fiber we impose[1]

$$\frac{L}{L_f} - \frac{L}{F_G} + 1 - \Theta_1 = 0, \tag{5}$$

and γ_1 and $B_1(\xi)$ reduce to [see Eq. (9), page 398 in Ref. 1 for details]

$$\begin{cases} \gamma_1 = -\frac{L}{L_f(\Lambda_1 + \Omega_G)}[\Lambda_1 \xi + i(1 - \overline{\Theta}_1 \xi)] \\ B_1(\xi) = L_f(1 - \overline{\Theta}_1 \xi + i\Omega_G \xi), \end{cases} \tag{6}$$

where $\overline{\Theta}_1 = 1 - \Theta_1$. Therefore, the exponential term can be expressed as

$$-i\frac{\kappa^2}{2\,k}[\gamma_1 B_1(\xi) - \gamma_1^* B_1^*(\xi)] = -\frac{L\kappa^2}{k(\Lambda_1 + \Omega_G)}[(1 - \bar{\Theta}_1 \xi)^2 + \Lambda_1 \Omega_G \xi^2], \tag{7}$$

and we obtain

$$\begin{aligned} T_{\text{focal}} &= -2 \cdot E_1(0{,}0)_f - E_2(0{,}0)_f \\ &= 4\pi^2 k^2 L \cdot \int_0^1 \int_0^\infty \kappa \cdot \Phi_n(\kappa) \cdot \left\{1 - \exp\left\{-\frac{L\kappa^2}{k(\Lambda_1 + \Omega_G)}[(1 - \bar{\Theta}_1 \xi)^2 + \Lambda_1 \Omega_G \xi^2]\right\}\right\}\mathrm{d}\kappa\,\mathrm{d}\xi. \end{aligned} \tag{8}$$

Note that if $L_f = F_G$, $\frac{L}{L_f} - \frac{L}{F_G} + 1 - \Theta_1 = 0$ gives $\Theta_1 = 1$, which means collimated beam incidents the collecting lens. For the general case of a beam not arriving collimated on the lens ($\Theta_1 \neq 1$), to insure the focusing on sensor/optical fiber, the distance behind the lens has to be $L_f = \frac{F_G \cdot L}{L + (\Theta_1 - 1) \cdot F_G}$. We remark that Eq. (3) diverges using the spectrum of Eq. (1) because outer scale is supposed to be infinite. However, it can be shown that such a singularity is removed in Eq. (8) and a finite result is found.

3.1 Kolmogorov Turbulence Case

Introducing Eq. (1) in Eq. (8) with $\alpha = 11/3$, we obtain the Kolmogorov turbulence case result for Gaussian beams

$$T_{\text{focal}} = 1.33 \cdot \sigma_R^2 \cdot (\Lambda_1 + \Omega_G)^{-\frac{5}{6}} \cdot \frac{8}{3} \cdot \int_0^1 \left[(1 - \bar{\Theta}_1 \xi)^2 + \Lambda_1 \Omega_G \xi^2\right]^{\frac{5}{6}} \mathrm{d}\xi, \tag{9}$$

where σ_R^2 is the Rytov variance.

For a beam arriving collimated on the collecting lens, $\Theta_1 = 1$, the integral in Eq. (9) can be expressed in closed form using the hypergeometric function ${}_2F_1(a, b; c, x)$ as

$$T_{\text{focal}} = 1.33 \cdot \sigma_R^2 \cdot (\Lambda_1 + \Omega_G)^{-\frac{5}{6}} \cdot \frac{8}{3} \cdot {}_2F_1\left(-\frac{5}{6}, \frac{1}{2}; \frac{3}{2}, -\Lambda_1 \Omega_G\right). \tag{10}$$

For a plane wave incident on the collecting lens, $(\Lambda_1 = 0, \Theta_1 = 1)$ we obtain

$$T_{\text{focal,pl}} = 1.33 \cdot \frac{8}{3} \cdot \sigma_R^2 \cdot \Omega_G^{-\frac{5}{6}} = 3.55 \cdot \sigma_R^2 \cdot \Omega_G^{-\frac{5}{6}}. \tag{11}$$

Finally, for a spherical wave incident on the collecting lens, $(\Lambda_1 = 0, \Theta_1 = 0)$ we obtain the same result as in Ref. 1

$$T_{\text{focal,sph}} = 1.33 \cdot \sigma_R^2 \cdot \Omega_G^{-\frac{5}{6}} = \left(\frac{D_G}{r_{0,\text{sph}}}\right)^{\frac{5}{3}}, \tag{12}$$

where $r_{0,\text{sph}} = (0.1623 \cdot C_n^2 \cdot k^2 \cdot L)^{-3/5}$ is the spherical Fried parameter.

For this specific spherical wave beam geometry, Andrews[1,3] modified Eq. (12) to include also the case when tip and tilt Zernike modes are both removed from the wavefront.

He introduced the coefficient 0.28 in the equation obtaining $T_{\text{focal,sph}_{[\text{tip-tilt corrected}]}} = 0.28 \cdot (D_G/r_{0,\text{sph}})^{\frac{5}{3}}$.

3.2 Non-Kolmogorov Turbulence Case

Using the non-Kolmogorov turbulence power spectrum, Eq. (1) we obtain

$$T_{\text{focal}}(\alpha) = \frac{1}{4}\frac{\alpha}{\sin(\alpha \cdot \frac{\pi}{4})} \cdot \tilde{\sigma}_R^2(\alpha) \cdot (\Lambda_1 + \Omega_G)^{1-\frac{\alpha}{2}} \cdot \int_0^1 \left[(1 - \bar{\Theta}_1\xi)^2 + \Lambda_1\Omega_G\xi^2\right]^{\frac{\alpha}{2}-1} \mathrm{d}\xi, \tag{13}$$

where $\tilde{\sigma}_R^2(\alpha) = -8\pi^2 \cdot \Gamma(1 - \frac{\alpha}{2}) \cdot \frac{1}{\alpha} \cdot \sin(\alpha \cdot \frac{\pi}{4}) \cdot A(\alpha) \cdot \tilde{C}_n^2 \cdot k^{3-\frac{\alpha}{2}} L^{\frac{\alpha}{2}}$ is the non-Kolmogorov Rytov variance defined in Ref. 2.

For a beam arriving collimated on the collecting lens, $\Theta_1 = 1$

$$T_{\text{focal}}(\alpha) = \frac{1}{4}\frac{\alpha}{\sin(\alpha \cdot \frac{\pi}{4})} \cdot \tilde{\sigma}_R^2(\alpha) \cdot (\Lambda_1 + \Omega_G)^{1-\frac{\alpha}{2}} \cdot {}_2F_1\left(1 - \frac{\alpha}{2}, \frac{1}{2}; \frac{3}{2}, -\Lambda_1\Omega_G\right). \tag{14}$$

For a plane wave incident on the collecting lens, $(\Lambda_1 = 0, \Theta_1 = 1)$ and we obtain

$$T_{\text{focal,pl}}(\alpha) = \frac{1}{4}\frac{\alpha}{\sin\left(\alpha \cdot \frac{\pi}{4}\right)} \cdot \tilde{\sigma}_R^2(\alpha) \cdot \Omega_G^{1-\frac{\alpha}{2}}. \tag{15}$$

For a spherical wave incident on the collecting lens, $(\Lambda_1 = 0, \Theta_1 = 0)$ and we obtain

$$T_{\text{focal,sph}}(\alpha) = \frac{1}{4} \cdot \frac{1}{\alpha - 1}\frac{\alpha}{\sin\left(\alpha \cdot \frac{\pi}{4}\right)} \cdot \tilde{\sigma}_R^2(\alpha) \cdot \Omega_G^{1-\frac{\alpha}{2}}. \tag{16}$$

Although we found expressions also for the non-Kolmogorov case, we show only results for Kolmogorov turbulence, $\alpha = 11/3$.

For a specific set of parameters, we plot in Fig. 2 the term T_{focal} as a function of the diffraction parameter, $\Lambda_0 = \frac{2L}{kW_0^2}$. Note that in our plots we change the spot size radius at the transmitter, W_0 from 0.001 m to 0.5 m covering the whole range from the near field $\Lambda_0 \ll 1$ to the far field $\Lambda_0 \gg 1$. The value $\Lambda_0 = 1$ corresponds to the value of $W_0 = \sqrt{\frac{2L}{k}} = \sqrt{\frac{\lambda L}{\pi}}$, which is the radius of the first Fresnel zone. Note also that for the case of a collimated beam, the value $\Lambda_0 = 1$ corresponds to the Rayleigh distance, $z_R = \frac{1}{2}kW_0^2$, which forms a separation line between the near and far field. All the following plots will show only results for collimated and focused beams because of their relevance to free space communications. In terms of the formalism used in this paper, it should be clear that the collimated beam at the transmitter has a wavefront radius of curvature $F_0 = \infty$; the focused beam has $F_0 = L$. Note furthermore that $F_0 = \infty$; $\Lambda_0 = 0$ is equivalent to the plane wave case at the transmitter and $F_0 = L; \Lambda_0 \to \infty$ is equivalent to the spherical wave case.

We deduce from Fig. 2 that for a collimated beam and for this set of parameters, the spread term T_{focal} is maximum in the near field. Note that in the region $\Lambda_0 \ll 1$ a collimated beam $(\Theta_0 = 1)$ is essentially a plane wave. This explains why the spread is higher: the radial dimension of the beam geometrically intercepts a higher number of turbulence cells along the path. The minimum value of T_{focal} is reached at about 2.5 times the Fresnel distance $(\Lambda_0 = 1)$ and, for $\Lambda_0 \gg 1$, T_{focal} increases up to the saturation value double than unity (it approaches the spherical wave case, $\Lambda_0 \to \infty, \Theta_1 \to 0$). On the other hand, a focused beam shows a lower spread than a collimated one all over the range from the near field to the far field, where it approaches again the

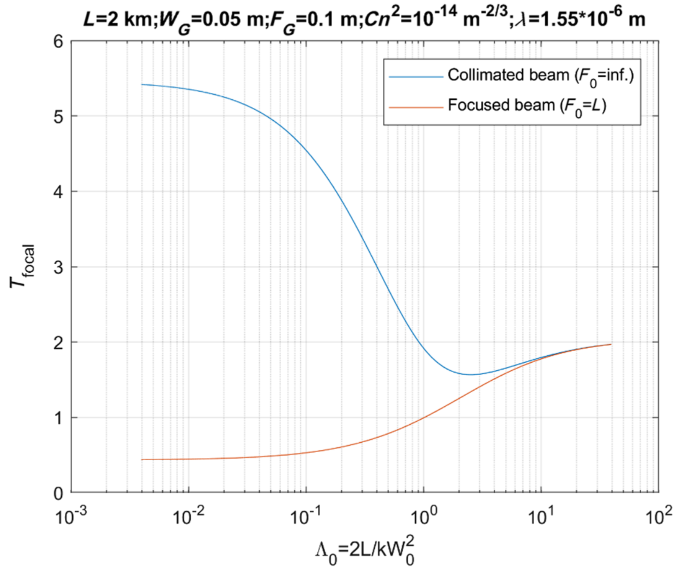

Fig. 2 Spread term T_{focal} as a function of the diffraction parameter Λ_0 for a beam collimated at the transmitter (blue) or focused on the receiver (red) (Kolmogorov turbulence case). Distance is fixed to the value $L = 2$ km.

spherical wave case $\Lambda_0 \to \infty, \Theta_0 = 0$. As for the collimated beam case, this is physically explained by the radial dimension of a focused beam, which intercepts a lower number of turbulence cells along the path.

In Fig. 3, we plot, for the collimated beam case, two spot radii in the focal plane, respectively, the long-term beam spread $W_{\mathrm{LT},f}$ and the diffraction limited spot radius W_2, both of them as a function of the diffraction parameter, $\Lambda_0 = \frac{2L}{kW_0^2}$. We deduce from Fig. 3 that in the near field $\Lambda_0 \ll 1$ (where plane wave model holds well) the long-term beam spread in the focal plane is higher than in the far field $\Lambda_0 \gg 1$, where the spherical wave model holds. This explains the saturation of both plots as well. Note also that the maximum diffraction-limited (no turbulence) spot radius W_2 can be obtained when the receiver is located at Fresnel distance, $\Lambda_0 = 1$.

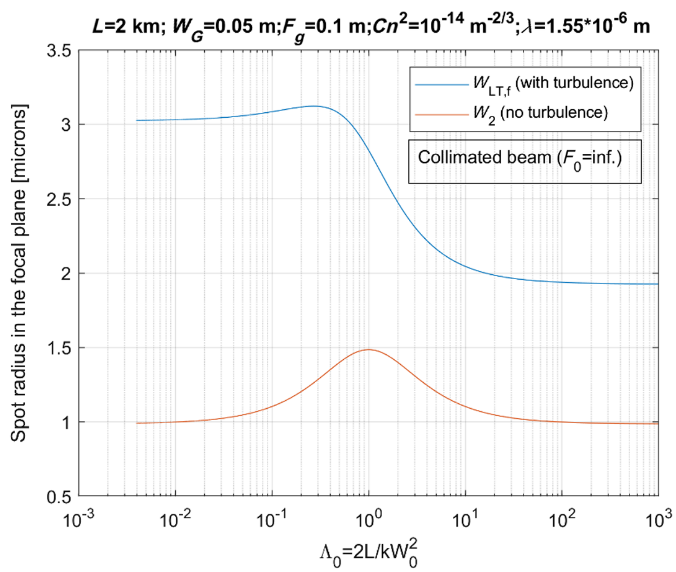

Fig. 3 Long-term beam spread term $W_{\mathrm{LT},f}$ (blue) and the diffraction limited spot radius W_2 (red) as a function of the diffraction parameter Λ_0 for a beam collimated at the transmitter (Kolmogorov turbulence case only). Distance is fixed to the value $L = 2$ km.

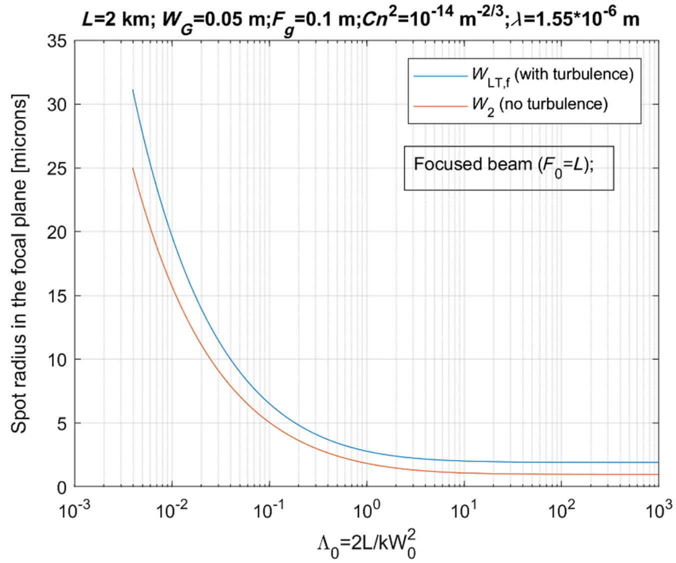

Fig. 4 Long-term beam spread term $W_{\mathrm{LT},f}$ (blue) and the diffraction limited spot size W_2 (red) as a function of the diffraction parameter Λ_0 for a beam focused on the receiver (Kolmogorov turbulence case). Distance is fixed to the value $L = 2$ km.

However, in turbulence it is more beneficial to locate the receiver in the far field to reduce the long-term spot size of the beam.

This conclusion also applies to a focused beam as shown in Fig. 4. Here we plot the same parameters as in Fig. 3 but now for a beam focused on the receiver. Note how the value of the long-term beam spread in the focal plane is essentially driven by the diffraction parameter $\Lambda_2 = \frac{L}{L_f} \cdot \frac{1}{\Lambda_1 + \Omega_G} = \frac{2L_f}{kW_2^2}$ or, in other words, it is anchored on the diffraction-limited spot size W_2.

To highlight the differences between the two beam geometries, we plot again in Fig. 5 the long-term beam spread in the focal plane $W_{\mathrm{LT},f}$ as a function of the diffraction parameter $\Lambda_0 = \frac{2L}{kW_0^2}$ for both a collimated and a focused beam (these two plots are the blue curves shown also in Figs. 3 and 4). We deduce from Fig. 5 that in the near field a collimated beam shows a lower long-

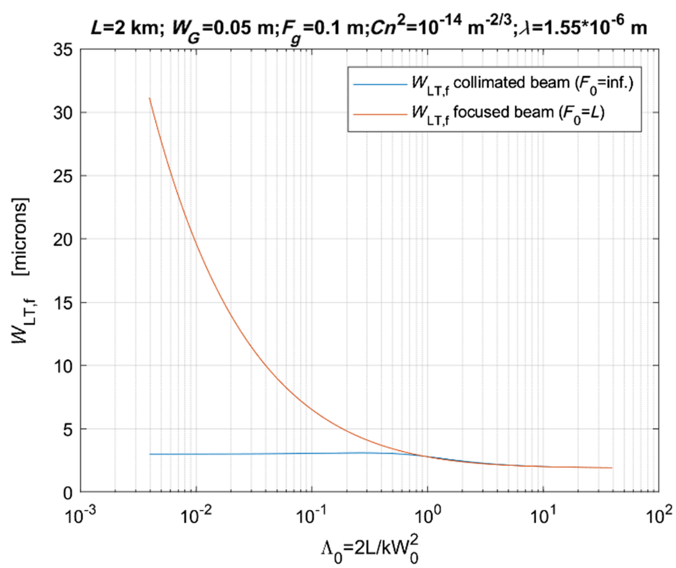

Fig. 5 Long-term beam spread term $W_{\mathrm{LT},f}$ as a function of the diffraction parameter Λ_0 for both beam geometries: collimated and focused (Kolmogorov turbulence case). Distance is fixed to the value $L = 2$ km.

term beam spread than a focused beam. However, they approach the same value when $\Lambda_0 = 1$ (Fresnel distance) or higher. In general, Fig. 5 suggests that independently from using a collimated or focused beam, to obtain the smallest long-term spot size in the focal plane the receiver should be located in the far field, $\Lambda_0 \gg 1$ (spherical wave model). We remark that in the far field Eq. (12) for spherical wave model holds well.

4 Strehl Ratio Analysis

The SR as one of the most used metrics at the focal plane is defined as[1]

$$SR = \frac{I_{\text{turb}}(0)}{I(0)}, \tag{17}$$

where $I(0)$ is the on-axis intensity in the focal plane of the beam after propagation in free space (no turbulence) and $I_{\text{turb}}(0)$ is the on-axis intensity of the beam in the focal plane after propagation in turbulence (we remark here that turbulence acts only from the transmitter to the receiver aperture, we neglect its effect behind the collecting lens). Using Eq. (9), the SR can be expressed as[1,3]

$$\text{SR} = \frac{1}{\left[1 + T_{\text{focal}}(\alpha)\right]^{\frac{6}{5}}}. \tag{18}$$

For the spherical wave case $(\Lambda_1 = 0, \Theta_1 = 0)$ and Kolmogorov turbulence, $\alpha = 11/3$, Eq. (18) reduces to the same result shown in Ref. 1 (see page 623)

$$\text{SR}_{\text{sph}} = \frac{1}{\left[1 + T_{\text{focal,sph}}\right]^{6/5}} = \frac{1}{\left[1 + 1.33 \cdot \sigma_R^2 \cdot \Omega_G^{-\frac{5}{6}}\right]^{6/5}} = \frac{1}{\left[1 + (D_G/r_{0,\text{sph}})^{5/3}\right]^{6/5}}. \tag{19}$$

We plot in Fig. 6 the SR as a function of the diffraction parameter $\Lambda_0 = \frac{2L}{kW_0^2}$ for the same scenario of propagation as previous plots. We deduce from Fig. 6 that using a focused beam and a receiver aperture located in the near field, $\Lambda_0 \ll 1$, is beneficial in terms of SR with respect to use a collimated beam. Physical conclusions are the same as those of Fig. 2. (The beam geometry defines the cross section of the beam while propagating through turbulence and focused beam intercepts a smaller number of turbulence cells than a collimated beam.)

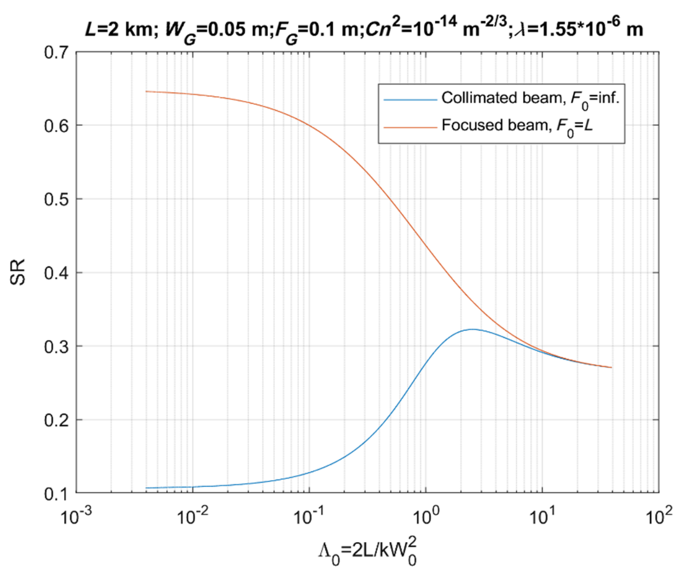

Fig. 6 SR as a function of the diffraction parameter Λ_0 for a beam collimated at the transmitter (blue) or focused on the receiver (red) (Kolmogorov turbulence case only). Distance is fixed to the value $L = 2$ km.

5 Power in the Bucket

The transmitted mean power of a Gaussian beam with peak intensity A_0^2 and spot radius W_0^2 is $P_{Tx} = \frac{1}{2}\pi A_0^2 W_0^2$ [Watt]. The fraction of the mean power entering the receiver aperture after propagation (distance L) is the PIB.[3] Considering a Gaussian lens (soft aperture) with radius W_G related to the hard aperture diameter, D_G by $W_G = \frac{D_G}{2\sqrt{2}}$ and supposing the turbulence affected beam still Gaussian,[1] the average $\langle \mathrm{PIB} \rangle$ can be expressed as

$$\langle \mathrm{PIB} \rangle = P_{Tx} \cdot \left[1 - e^{-2\left(\frac{W_G}{W_{\mathrm{LT,pupil}}}\right)^2} \right] \text{[Watt]}, \tag{20}$$

where we ignored the atmospheric transmission loss caused by aerosols, etc., and the receiver optical element transmission loss.

For a large beam (close to a plane wave) incident on the lens, an approximation is[3]

$$\langle \mathrm{PIB} \rangle_{W_{\mathrm{LT_{pupil}}} \gg W_G} \cong P_{Tx} \cdot \left(\frac{W_G}{W_{\mathrm{LT,pupil}}} \right)^2 = P_{Tx} \cdot \left(\frac{W_G}{W} \right)^2 \cdot \frac{1}{\left[1 + T_{\mathrm{pupil}}(\alpha) \right]^{\frac{6}{5}}}, \tag{21}$$

where $W_{\mathrm{LT,pupil}} = W[1 + T_{\mathrm{pupil}}(\alpha)]^{\frac{3}{5}}$ is the long term beam spread at the receiver aperture, W is the diffraction limited spot radius at distance L; and $T_{\mathrm{pupil}}(\alpha) = \frac{1}{4}\frac{\alpha}{\alpha-1}[\sin(\alpha\frac{\pi}{4})]^{-1}\Lambda^{\frac{\alpha}{2}-1}\tilde{\sigma}_R^2(\alpha)$ is the analogous of $T_{\mathrm{focal}}(\alpha)$ at the receiver (pupil) aperture (see Refs. 1 and 2). Note that for Kolmogorov turbulence $T_{\mathrm{pupil}}(\alpha = \frac{11}{3}) = 1.33 \cdot \sigma_R^2 \cdot \Lambda^{\frac{5}{6}}$.

We plot in Figs. 7 and 8 the percentage of PIB scaled by the transmitted power, P_{Tx} as a function of the diffraction parameter Λ_0 for several distances of the receiver for a collimated beam at the transmitter or focused on the receiver (Kolmogorov turbulence case only). We deduce from Figs. 7 and 8 that the maximum PIB is reachable when the beam is focused on the receiver (see Fig. 8) and the collecting lens is located in the near field. Also, when the receiver is positioned in the far field the spherical wave model [please see Eqs. (12) and (19)] holds well and there is essentially no difference in using either beam geometry.

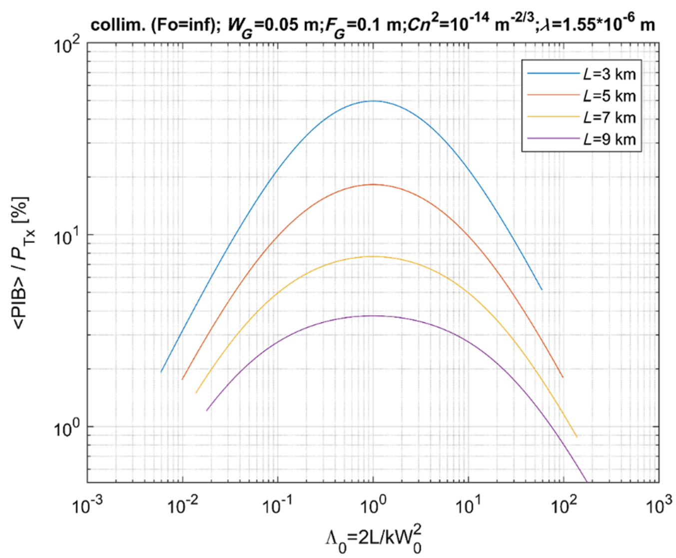

Fig. 7 Percentage of PIB scaled by the transmitted power as a function of the diffraction parameter Λ_0 for several distances of the receiver for a collimated beam at the transmitter (Kolmogorov turbulence case only).

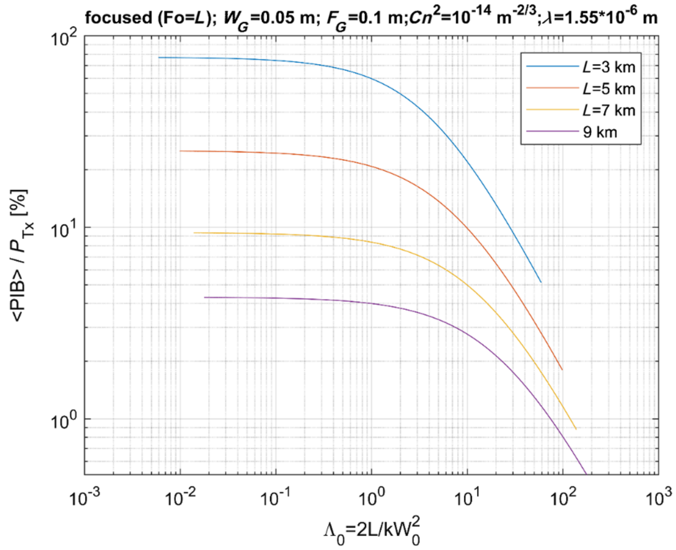

Fig. 8 Percentage of PIB scaled by the transmitted power as a function of the diffraction parameter Λ_0 for several distances of the receiver for a beam focused on the receiver (Kolmogorov turbulence case only).

6 Power over the Sensor

Similar to the PIB but now on the focal (detector) plane, the fraction of transmitted mean power illuminating the sensor/detector (POS) can be expressed as

$$\langle \mathrm{POS} \rangle = \langle \mathrm{PIB} \rangle \cdot \left[1 - e^{-2 \cdot \left(\frac{W_S}{W_{LT,f}} \right)^2} \right], \tag{22}$$

where W_S is the radius of the sensor (supposing it has a circular geometry) and, as previously mentioned, we ignored any additional loss, such as circulator loss and optical loss.[3]

Supposing the beam illuminating the sensor is consistently larger than the sensor itself (the Gaussian beam across the sensor is almost a plane wave), an approximated expression of Eq. (22) is

$$\begin{aligned} \langle \mathrm{POS} \rangle_{W_{\mathrm{LT},f} \gg W_{\mathrm{sensor}}} &\cong \langle \mathrm{PIB} \rangle \cdot \left(\frac{W_S}{W_{\mathrm{LT},f}} \right)^2 = \langle \mathrm{PIB} \rangle \cdot \left(\frac{W_S}{W_2} \right)^2 \cdot \frac{1}{\left[1 + T_{\mathrm{focal}}(\alpha) \right]^{\frac{6}{5}}} \\ &= \langle \mathrm{PIB} \rangle \cdot \left(\frac{W_S}{W_2} \right)^2 \cdot \mathrm{SR}_{\mathrm{focal}}[\mathrm{Watt}]. \end{aligned} \tag{23}$$

We plot in Figs. 9 and 10, respectively, the percentage of POS scaled by the transmitted power, P_{Tx} as a function of the diffraction parameter Λ_0 for several distances of the receiver for a collimated beam at the transmitter and for a beam focused on the receiver (Kolmogorov turbulence case only).

We deduce from Figs. 9 and 10 that, for both geometries and for this specific set of parameters, the maximum POS is reachable when Λ_0 assumes values in the interval from two to five times the Fresnel distance ($\Lambda_0 = 1$), depending on path distances (note that the peak shifts slightly to the left at shorter distances). Also, there is essentially no difference of using the two different beam geometries (collimated or focused beam) in the far field (spherical wave model holds well in such a case).

7 Power into the Fiber

Supposing an optical fiber positioned in the focal plane, the mean power coupled into the fiber can be expressed as[3]

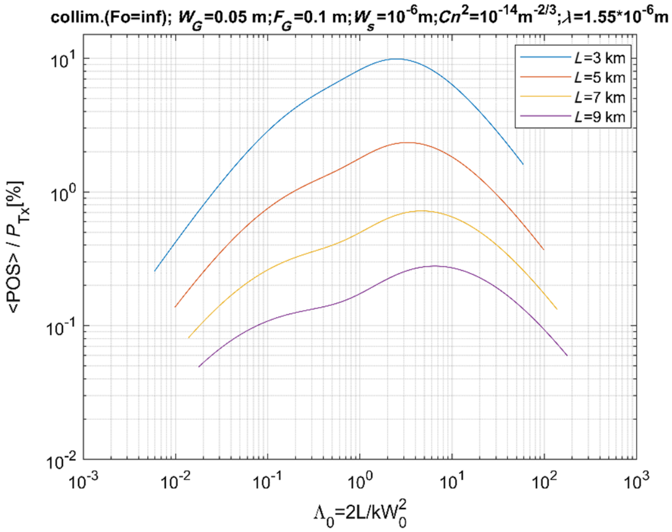

Fig. 9 Percentage of POS scaled by the transmitted power as a function of the diffraction parameter Λ_0 for several distances of the receiver for a collimated beam at the transmitter (Kolmogorov turbulence case only).

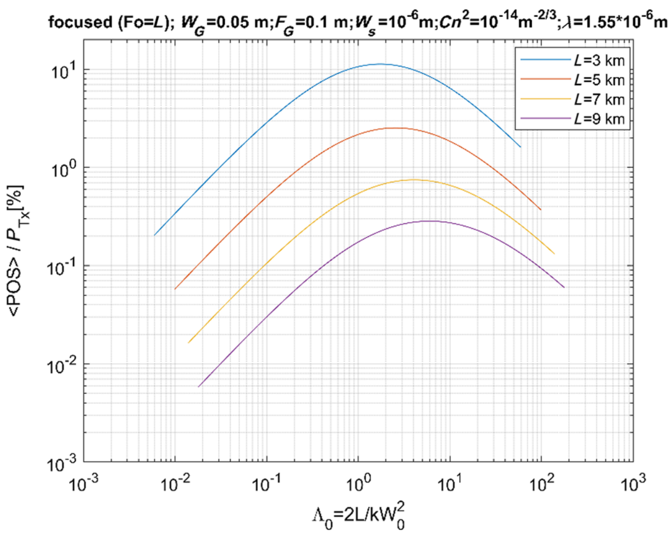

Fig. 10 Percentage of POS scaled by the transmitted power as a function of the diffraction parameter Λ_0 for several distances of the receiver for a beam focused on the receiver (Kolmogorov turbulence case only).

$$\langle \mathrm{PIF} \rangle = \langle \mathrm{PIB} \rangle \cdot \eta \cdot SR_{\mathrm{focal}} = \langle \mathrm{PIB} \rangle \cdot \eta \cdot \frac{1}{\left[1 + T_{\mathrm{focal}}(\alpha)\right]^{\frac{6}{5}}} = \langle \mathrm{PIB} \rangle \cdot \eta_{\mathrm{turb}} \ [\mathrm{Watt}], \tag{24}$$

where $\eta_{\mathrm{turb}} = \eta \cdot \mathrm{SR}_{\mathrm{focal}}$, η_{turb} is the fiber coupling efficiency including the turbulence-induced beam spread (it includes the reduction of power due to turbulence effects in focal plane, $\mathrm{SR}_{\mathrm{focal}}$) and η is the free space (defined without keeping into account the turbulence) fiber coupling efficiency. In our analysis, as already mentioned, we ignored any additional loss such as circulator loss and optical loss.[3]

We plot in Figs. 11 and 12 the PIF as a function of the diffraction parameter Λ_0 for several distances of the receiver for a collimated beam at the transmitter or for a beam focused on the receiver (Kolmogorov turbulence case only). Similar to the POS in Fig. 9, we deduce from Fig. 11 (collimated beam) that, for this specific set of parameters, the maximum PIF is reachable

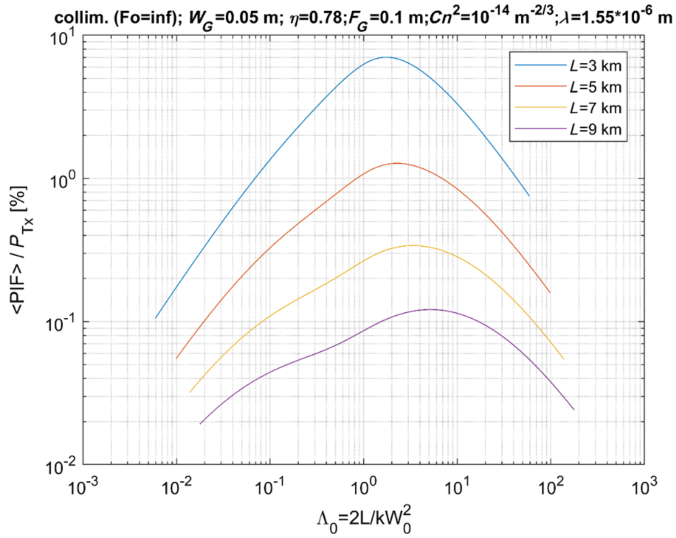

Fig. 11 Percentage of PIF scaled by the transmitted power as a function of the diffraction parameter Λ_0 for several distances of the receiver for a collimated beam at the transmitter (Kolmogorov turbulence case only).

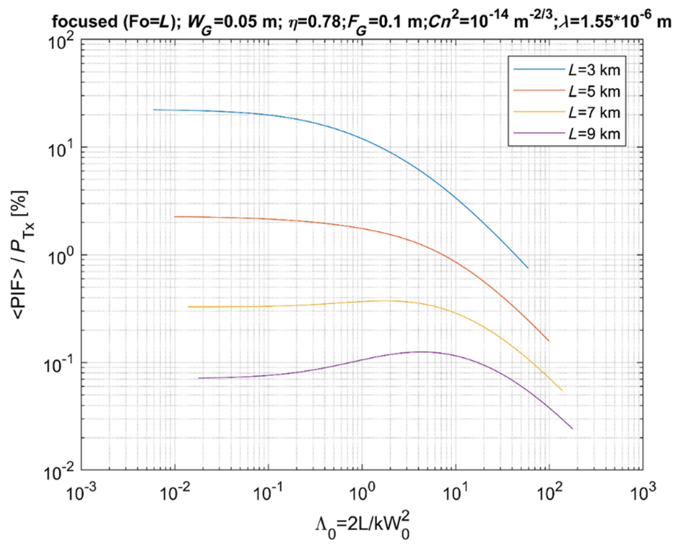

Fig. 12 Percentage of PIF scaled by the transmitted power as a function of the diffraction parameter Λ_0 for several distances of the receiver for a beam focused on the receiver (Kolmogorov turbulence case only).

when Λ_0 assumes values in the interval from two to five times the Fresnel distance $(\Lambda_0 = 1)$, depending on path distances (note that the peak shifts slightly to the left at shorter distances).

Also, when the beam is focused on the receiver, we deduce form Fig. 12 that the maximum PIF (for this specific set of parameters) is reached mostly in the near field. Finally, similarly to previous metrics, we note that when the receiver is located in the far field the spherical wave model holds well and there is essentially no difference in using either beam geometry (collimated or focused beam case).

8 Conclusion

In this paper, we used the ABCD matrix formulation to obtain the analytical expressions of the main optical power-related metrics for a Gaussian beam after propagation through atmospheric turbulence. Specifically, these optical power-related metrics are: the long-term beam spread in the focal plane, SR, PIB, POS, and PIF. We investigated those metrics as a function of the diffraction parameter, $\Lambda_0 = \frac{2L}{kW_0^2}$.

For a specific set of parameters, we found that both the maximum SR and PIB are reachable when a beam focused on the receiver is used and the collecting lens is located in the near field. In addition, we found that for a collimated beam the maximum POS and PIF are reachable when the diffraction parameter Λ_0 assumes values in the interval two to five times the Fresnel distance $(\Lambda_0 = 1)$ depending on path distances (the POS and PIF peaks shifts slightly to the left at shorter distances). However, when the beam is focused on the receiver, the maximum PIF is mostly reached in the near field.

Finally, in the far field and for all metrics analyzed in this paper, the spherical wave model holds well and there is essentially no difference of using the two different beam geometries (collimated or focused beam). Our results can be useful for the budget link analysis for free space optical communications.

Code and Data Availability

The data that support the findings of this study are available from the corresponding author upon reasonable request.

Acknowledgments

This work was sponsored by WTD 91 (Technical Center of Weapons and Ammunition) of the Federal Defence Forces of Germany—Bundeswehr in the project ABU-SLS. The author would like to thank Dr. Szymon Gladysz, co-author of Ref. 4, on which this paper is mainly based.

References

1. L. C. Andrews and R. L. Phillips, *Laser Beam Propagation through Random Media*, 2nd ed., SPIE Optical Engineering Press, Bellingham, WA (2005).
2. I. Toselli et al., "Free space optical system performance for a Gaussian beam propagating through non-Kolmogorov weak turbulence," *IEEE Trans. Antenn. Propag.* **57**(6), 1783–1788 (2009).
3. L. C. Andrews, *Field Guide to Atmospheric Optics*, SPIE Filed Guide, Vol. **FG41**, 2nd ed., SPIE Press (2019).
4. I. Toselli and S. Gladysz, "Long-term beam size analysis in the focal plane for atmospheric turbulence-affected laser beams," *Proc. SPIE* **12237**, 122370A (2022).

Dr. Italo Toselli is the founding member of TurbOttica LLC and a senior scientist at Fraunhofer IOSB. For more than 15 years, his research has focused on laser beam propagation through atmospheric and oceanic turbulence. He is a reviewer of main journals in optics and atmospheric propagation, and he has served as invited speaker at SPIE and Optica (former OSA) conferences. He is a senior member of Optica, an instructor of SPIE, and a committee member of main conferences in his field.